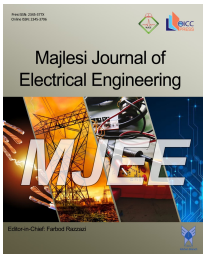

Volume 18, Issue 2, 182431 (1-11)

Majlesi Journal of Electrical Engineering (MJEE)

https://dx.doi.org/10.57647/j.mjee.2024.1802.31

An optimized closed-loop Z-source inverter for wind energy generation system using opposition-based sine cosine algorithm

Sweta Kumari*, Rajib Kumar Mandal

National Institute of Technology/Electrical Engineering, Patna, India.

***Corresponding author:** swetak.phd18.ee@nitp.ac.in

Original Research

Received:
13 February 2024
Revised:
23 March 2024
Accepted:
1 May 2024
Published online:
11 May 2024

Abstract:

For transformer-less operation, a wind energy generating system (WEGS) with an 8.5 kW wind turbine and a 6.6 kW Z-source inverter (ZSI) is modelled. A closed-loop control technique is employed at the load side of the WEGS to obtain a constant voltage with a fluctuating load at the output side of the system. The ZSI is used with a proportional-integral (PI) controller for closed-loop control since it is the least complicated controller to operate and tune. As an effect of ZSI's nonlinear nature, PI controllers cannot be used directly with this system. The primary focus of this study is the optimization of stabilized PI coefficients (Kp, Ki). PI tuning for closed-loop ZSI is taken care of with the use of particle swarm optimization (PSO), the sine-cosine algorithm (SCA), and the opposition-based sine-cosine algorithm (OB-SCA). The OB-SCA provides superior closed-loop ZSI stability when used with WEGS. MATLAB is used for both the design and simulation of the system. The results demonstrate that the proposed controller can precisely regulate the AC output voltage of ZSI with WEGS.

Keywords: Opposition-based sine-cosine algorithm (OB-SCA); Proportional-integral (PI) controller; Wind energy generation system (WEGS); Z-source inverter (ZSI).

1. Introduction

The ongoing scene faces difficulties in diminishing greenhouse impacts and further developing energy effectiveness. Renewable energy (RE) is the best elective method for dealing with this issue. Thus, numerous nations have put forth a few attempts to determine this issue [1]. They have considered a reasonable and productive arrangement, which depends on RE sources. RE is a clean energy source that creates power without emitting ozone-depleting substances. Distributed electricity generation also mainly involves the use of RE sources [2]. Currently, RE sources account for between 15% and 20% of total global energy interest. Over 70% of the RE is being produced by wind energy [3].
Because of the rising need for electricity in modern times, RE sources are necessary. For this reason, researchers are working to create an affordable WEGS system with fewer components, less complexity, and more input power consumption. In addition to designing an optimal controller for closed-loop operation, this study develops an optimized closed-loop WEGS model that eliminates the need for an extra boost component, making the WEGS model more cost-effective. Reduced switching losses and high DC input utilization are the main goals of the SV-PWM technology. As a result, the suggested WEGS model's overall performance improved.
Between the wind turbine generator and load center in WEGS, an interference power electronic converter is required. With traditional WEGS, the wind turbine is connected to a permanent magnet synchronous generator (PMSG), a three-phase rectifier, a three-phase conventional inverter, and transformers to boost or buck the energy level at the load centers. It lessens the system's overall efficiency and adds to its weight, volume, cost, and complexity [4]. Also, there is a requirement for high-performance boost-type inverters because RE sources have low DC voltage output. ZSI is a single-stage power converter that is capable of both bucking and boosting [5]. In Fig. 1, the ZSI model

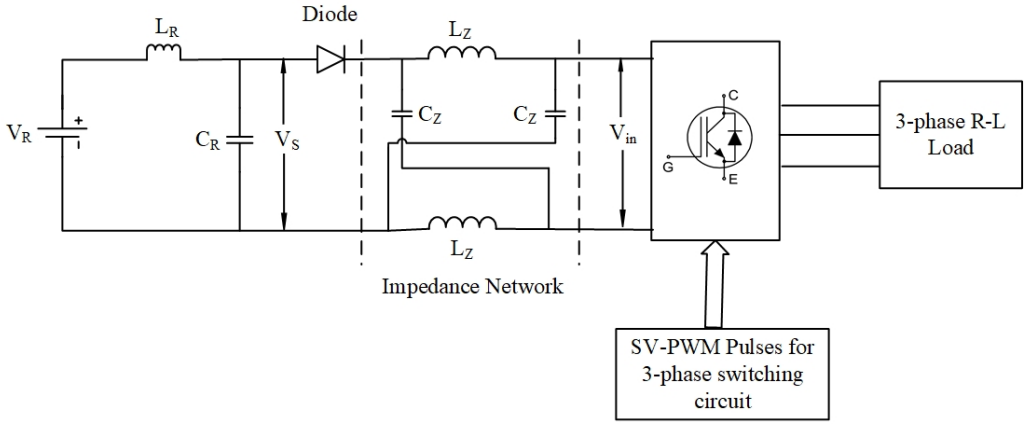

Figure 1. Open-loop ZSI model with DC input voltage and RL-load.

is displayed, whose input supply is rectifier DC voltage (V_R) with an L-C filter (L_R-C_R). In the ZSI, it is possible to turn on both switches in a phase leg at once (shoot-through state of operation). The ZSI's impedance network with two inductors and two capacitor components makes a shoot-through (ST) state conceivable for the ZSI. By eliminating the dead time in the switching pattern, this special feature reduces output waveform distortion and increases reliability [6]. The ZSI may offer voltage buck and boost capabilities in a single stage of power conversion with increased output voltage range, improved power factor, reliability, lower cost, and decreased line harmonics by regulating the modulation index and ST duty ratio [4].

ZSI has a lot of advantageous features; however, its effectiveness is mostly determined by the following control methods: feedback control and modulation strategy [7]. There are numerous works in which the issue is considered a controlling variable. PID and PI controllers are commonly used for regulating the capacitor voltage of ZSI's impedance network. Due to this, PI and PID controllers have been the subject of extensive research [8–10]. The PI controller appears to have a straightforward operation that is easy to comprehend. Engineers continue to favor the PI controller for ZSI control operation as there are only two design parameters, namely Kp (proportional) and Ki (integral) [11]. Despite being an effective control method, the development of PI's parameters for ZSI structures is a fascinating subject (Miyani, P.B., Sant, 2022). In addition, ZSI systems' nonlinear nature limits the direct application of this control method [12]. However, research in the above literature does not primarily focus on finding the optimal values for the controller parameters. Computing the parameters for a PI or PID controller is viewed as an optimization challenge. By adjusting the control parameters, optimized PI control helps ZSI to operate as efficiently as possible. This minimizes conversion process losses and results in improved input power usage. In transients, the PI control optimization helps to provide quicker and more precise reactions. The genetic algorithm [13], particle swarm optimization (PSO) [14], and other heuristic techniques [15] are used to determine these values. However, these optimization methods cannot be used for non-linear ZSI control.

As closed-loop ZSI for constant voltage at the output side needs an optimization technique for the optimal value of proportional and integral parameters, some conventional optimization algorithms are tested on it for the closed-loop stable system. Although PSO has the advantage of being simple to implement, it also has disadvantages for power system applications such as premature convergence, difficulties handling limitations, and a high computing cost [16]. Another optimization technique utilized for PI parameter control is the sine-cosine algorithm (SCA). The sine and cosine functions are the sources of inspiration for the SCA. It is a metaheuristic optimization algorithm. For the search process, exploration and exploitation can be successfully balanced in the SCA. Fast convergence, easy implementation, and excellent accuracy are further benefits of SCA. Thus, the SCA is a quick and effective optimization technique that may offer precise solutions to a variety of optimization issues [17]. While the SCA offers several benefits, it also has certain drawbacks in terms of finding local optima that should be taken into account when choosing an optimization method for a specific task [18, 19]. Thus, in this article, for the optimization process, a modified version of SCA, named OB-SCA, is used, which has all the benefits of SCA but has a double particle value so that there is no risk of a local optimum occurring and will reach the global optimum value in a smaller iteration number.

As far as the author is concerned, the close-loop controlled ZSI model with WEGS is no longer intended for constant output voltage with varying loads using the optimal value of controlled parameters.

This article proposes a newly developed optimization technique, OB-SCA, for the stable operation of a closed-loop ZSI model working in WEGS. The Z-source inverter's closed-loop control allows for real-time feedback and adjustment. The system can adjust to changing operational conditions when coupled with an optimization technique, guaranteeing stability and best performance in dynamic scenarios like fluctuating loads. Decisions based on load current system states can be made in real-time using the closed-loop system and an optimization technique. Thus, this paper's most important contributions are summarized below:

1- A WEGS model is simulated with a specific wind turbine, PMSG, and ZSI parameters.
2- A transfer function for ZSI's capacitor voltage and ST duty cycle is developed for the ZSI closed-loop operation by state-space analysis of the ZSI model.
3- A ZSI's proper modulation approach is discovered and applied to it to reduce THD at the inverter's AC output side.
4- A flowchart for determining the optimum controller parameters is mapped after the analysis of the OB-SCA optimization technique.
5- The system's responsiveness with the PI controller is examined.
The following sections comprise the remaining text of this article: section 2 presents the proposed WEGS structure. The modulation strategy for the 3-phase switching circuit of the ZSI is discussed in section 3. Section 4 depicts the state-space analysis of ZSI for determining the transfer function of ZSI's capacitor voltage and ST duty ratio, which contribute to the controller design. In section 5, the proposed optimization technique is discussed in detail for finding the optimal proportional and integral parameters of a PI controller. In section 6, the relevant results of the proposed WEGS system are dealt with, which is the result and discussion section. The summary of this article is concluded in section 7.

2. Proposed WEGS model

The proposed WEGS design with load-side control is shown in Fig. 2. A wind turbine, a PMSG, a three-phase rectifier, a rectifier L-C filter, a ZSI, an inverter L-C filter, and a load-side control controller make up this system. In a single stage, ZSI is used to buck or raise the voltage level. The continuous DC voltage input to the ZSI is provided by the rectifier output capacitor voltage. Moreover, harmonics created in the AC output by the PWM process are reduced using the inverter L-C filter.

3. Space vector pulse width modulation (SVPWM)

When designing a controller, modulation techniques must also be taken into account. If the proper modulation technique is not selected, significant voltage stress on switches with low efficiency and high total harmonic distortion (THD) is highly probable to occur [20]. For a three-phase ZSI system, many PWM techniques are employed. According to the literature [21, 22], SV-PWM is the most suitable modulation approach for a three-phase ZSI in terms of the percentage of THD that occurs at the AC output side of the system.
Fig. 3 depicts the controlled SV-PWM approach strategy for closed-loop ZSI operation using the block diagram proposed in this article.

So, the ZSI can raise the voltage to the AC output that is needed [23]. The modulation parameters are shown in Table 1.

4. State-space analysis of ZSI

The ZSI has the modulation index and the ST duty ratio for controlling the inverter, unlike conventional inverters, which only have the modulation index. Thus, the ZSI can simultaneously regulate the capacitor voltage and output voltage. The equivalent model of the ZSI is shown in Fig. 4. For the equivalent circuit to be modelled, the following assumptions are made: The two inductors' currents and the voltage across the capacitors are always equal since the Z-source impedance circuit is symmetrical. On the basis of this supposition, three state variables exist:
(i) Inductor current (i_{LZ}) (ii) Capacitor voltage (v_{CZ}) (iii) Load current (i_{Load}) The duty ratios of S_1 and S_2, shown in Fig. 5, are D_{st} (ST duty ratio) and M (modulation index), respectively.

$$\begin{bmatrix} si_{LZ} \\ sv_{CZ} \\ si_{Load} \end{bmatrix} = \begin{bmatrix} 0 & -\frac{1}{L_Z} & 0 \\ \frac{1}{c} & 0 & -\frac{1}{C_Z} \\ 0 & \frac{2}{L_{Load}} & -\frac{R_{Load}}{L_{Load}} \end{bmatrix} \begin{bmatrix} i_{LZ} \\ v_{CZ} \\ i_{Load} \end{bmatrix} + \begin{bmatrix} \frac{V_S}{L_Z} \\ 0 \\ \frac{-V_S}{L_{Load}} \end{bmatrix} \quad (1)$$

When in the ST state (S_1 is on S_2 is off), the state equation is shown in (2). This state has a duty ratio of D_{st}.

$$\begin{bmatrix} si_{LZ} \\ sv_{CZ} \\ si_{Load} \end{bmatrix} = \begin{bmatrix} 0 & \frac{1}{L_Z} & 0 \\ -\frac{1}{c} & 0 & 0 \\ 0 & 0 & -\frac{R_{Load}}{L_{Load}} \end{bmatrix} \begin{bmatrix} i_{LZ} \\ v_{CZ} \\ i_{Load} \end{bmatrix} \quad (2)$$

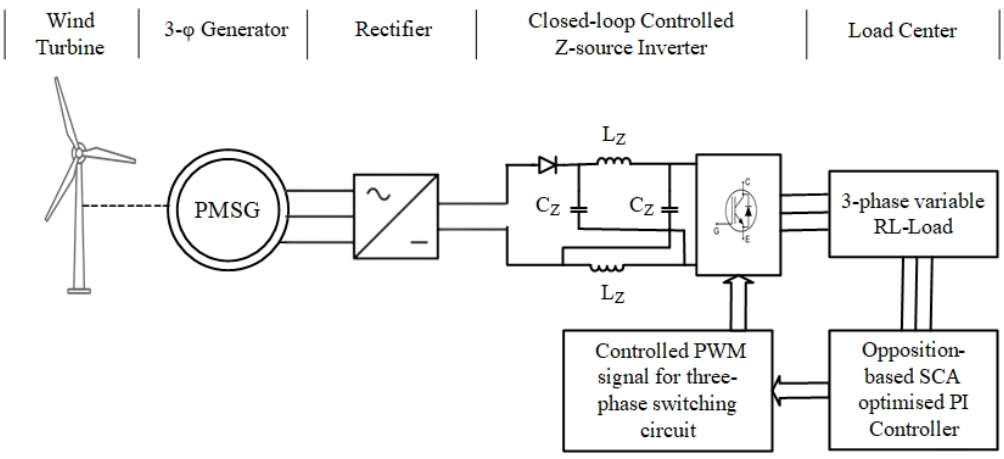

Figure 2. Proposed WEGS model with variable RL-load.

Table 1. SV-PWM parameters

Parameters	Value
Reference Wave Amplitude	1 V
Carrier Wave Frequency	1000 Hz
DC Input Voltage	120 V
Reference Voltage	(2/3)×120×0.3
Switching Frequency	50 Hz
Duty Ratio for ZSI, D_{st}	0.3
Modulation Index, M	0.7
Boost Factor	2.5

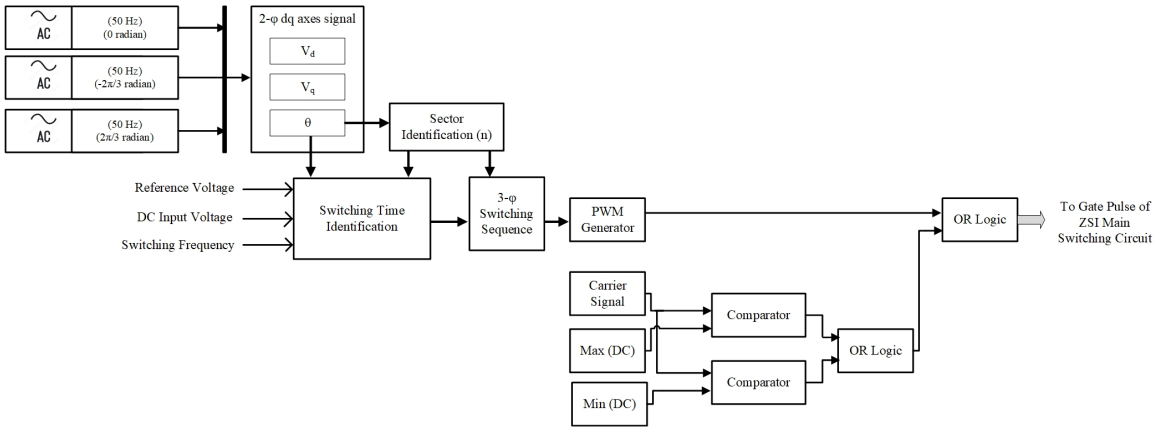

Figure 3. SV-PWM technique for proposed system.

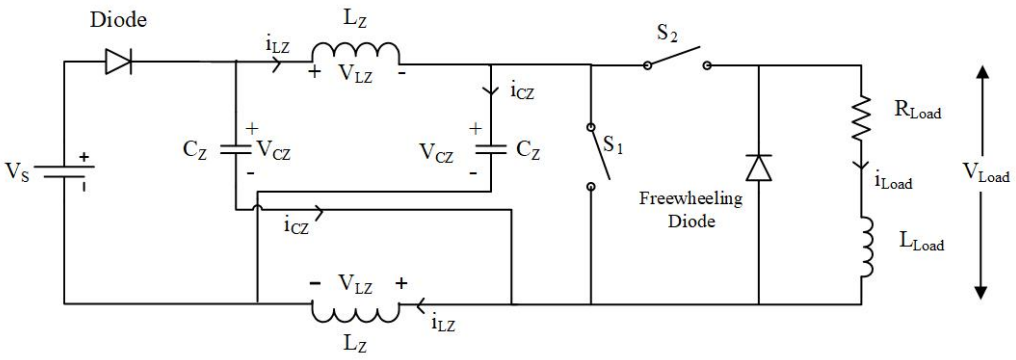

Figure 4. ZSI equivalent model.

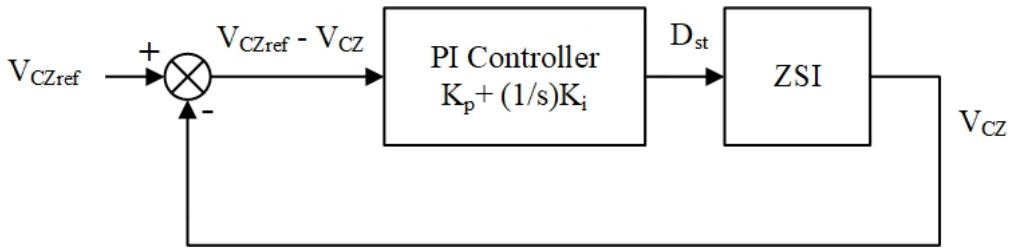

Figure 5. ZSI control technique with PI controller for variable AC load.

When in the zero state (S_1 is off S_2 is off), the state equation is shown in Equation (3). This state has a duty ratio of (1-D_{st}-M).

$$\begin{bmatrix} si_{LZ} \\ sv_{CZ} \\ si_{Load} \end{bmatrix} = \begin{bmatrix} 0 & -\frac{1}{L_Z} & 0 \\ \frac{1}{c} & 0 & 0 \\ 0 & 0 & -\frac{R_{Load}}{L_{Load}} \end{bmatrix} \begin{bmatrix} i_{LZ} \\ v_{CZ} \\ i_{Load} \end{bmatrix} + \begin{bmatrix} \frac{V_S}{L_Z} \\ 0 \\ 0 \end{bmatrix} \tag{3}$$

The model of the system developed using (1).M + (2). D_{st} + (3). (1-D_{st}-M) is shown in Equation (4).

$$\begin{bmatrix} si_{LZ} \\ sv_{CZ} \\ si_{Load} \end{bmatrix} = \begin{bmatrix} 0 & \frac{2D_{st}-1}{L_Z} & 0 \\ \frac{1-2D_{st}}{C} & 0 & -\frac{M}{C_Z} \\ 0 & \frac{2M}{L_{Load}} & -\frac{R_{Load}}{L_{Load}} \end{bmatrix} \begin{bmatrix} i_{LZ} \\ v_{CZ} \\ i_{Load} \end{bmatrix} + \begin{bmatrix} \frac{V_S}{L_Z}(1-D_{st}) \\ 0 \\ -\frac{V_S}{L_{Load}}M \end{bmatrix} \tag{4}$$

The state space model can be used to derive the following equations that describe the steady state of state variables:

$$\begin{cases} I_{LZ} = \frac{1-D_{st}}{1-2D_{st}} I_{Load} \\ V_{CZ} = \frac{1-D_{st}}{1-2D_{st}} V_S \\ I_{Load} = \frac{V_{CZ}}{R_{Load}} \end{cases} \tag{5}$$

When the second order is not taken into consideration, Equation (4) can be simplified through small signal analysis $u(t) = U + \tilde{u}(t)$. In order to obtain a model of the state space, equilibrium points are used that have already been determined (I_{LZ}, V_{CZ}, I_{Load}, D_{st}, M) along with the perturbations of state variables ($\tilde{i}_{LZ}, \tilde{V}_{CZ}, \tilde{i}_{Load}, \tilde{D}_{st}, \tilde{M}$).

$$\begin{cases} \tilde{si}_{LZ} = \frac{2D_{st}-1}{L_Z}\tilde{V}_{CZ} + \frac{2V_{CZ}-V_S}{L_Z}\tilde{D}_{st} \\ \tilde{sv}_{CZ} = \frac{1-2D_{st}}{C_Z}\tilde{i}_{LZ} - \frac{M}{C_Z}\tilde{i}_{Load} - \frac{2I_{LZ}}{C_Z}\tilde{D}_{st} - \frac{I_{Load}}{C_Z}\tilde{M} \\ \tilde{si}_{Load} = \frac{2M}{L_{Load}}\tilde{V}_{CZ} - \frac{R_{Load}}{L_{Load}}\tilde{i}_{Load} + \frac{2v_{CZ}-V_S}{L_{Load}}\tilde{M} \end{cases} \tag{6}$$

The transfer functions at any particular operating point can be obtained by solving steady-state equations with a small signal. Fig. 5 depicts the control blocks for a ZSI.
Hence, from the state space model, the third-order transfer function yields the ZSI transfer function, shown in Equation (7).

$$T\frac{v_{CZ}}{D_{st}}(s) = \frac{\tilde{v}_{cz}(s)}{\tilde{D}_{st}(s)} | at \tilde{v}_s(s) = \frac{(-2I_{LZ}+I_{Load})L_Z L_{Load}s^2 + (-2I_{LZ}+I_{Load})L_Z R_{Load}}{A} \tag{7}$$

where,

$$A = L_Z C_Z L_{\text{Load}} S^3 + L_Z C_Z R_{\text{Load}} S^2 + (2M^2 L_Z + (D_{st}-M)^2 L_{\text{Load}})S + (D_{\text{st}}-M)^2 R_{\text{Load}} \text{ and, } V_0 = 2V_{\text{CZ}} - V_{\text{S}} \tag{8}$$

After an adequate model of the system has been derived, it must meet certain performance characteristics, including reference tracking, stability, and durability against any unexpected events. The goal of this research paper is to come up with a PI control law for ZSI. When it comes to the ZSI, the control variable is the ST-duty ratio (D_{st}).
This PI controller is what produces the switching pulses. Fig. 6 depicts the modulation strategy for regulating the capacitor voltage and ST duty cycle. The typical modulation scheme is enhanced to acquire the transfer function of V_{CZ}/D_{st} for controller design purposes. Parameter optimization for the controller, a critical task for ZSI applications, is the focus of the next section, which employs OB-SCA-based methodologies.

5. Opposition-based SCA

Using mathematical functions like sine and cosine, the Sine-Cosine Algorithm (SCA) is an evolutionary optimization approach that discovers the best answer to a problem. This method was first presented in [24], and it has subsequently been applied to issues like global optimization, multi-objective optimization, and feature selection [25–27].

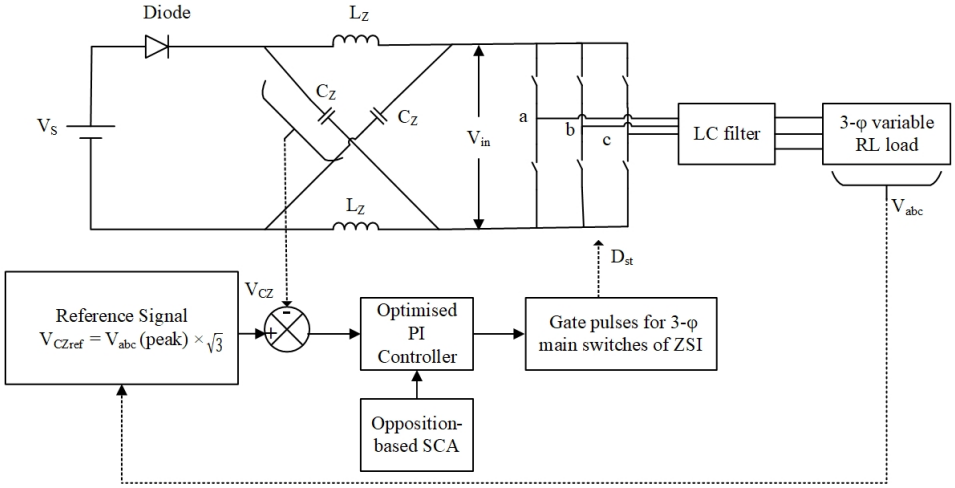

Figure 6. Optimization-based closed-loop control of ZSI with variable RL-load.

SCA has a high rate of convergence and generates high-quality solutions, making it a popular choice among optimization techniques [28].

Proposed OB-SCA technique: Because the conventional SCA position updating path has an absolute value item, it is easy for the traditional SCA to get stuck in the early phase of the algorithm and have trouble finding the global optimum. This is especially true for highly nonlinear and very ill-posed problems. The algorithm's search direction cannot be well limited by the search path. Additionally, traditional SCA's convergence speed will slow down as the number of dimensions goes up. This article shows how to enhance the performance of standard SCA by using an empirical parameter and a linear search path to make it more capable of conducting a global search and finding a stable optimal solution. Opposition-based learning (OBL) is incorporated into the optimization procedure of OB-SCA [29], a kind of SCA. In an opposition-based approach, all possible solutions from the population are compared to the optimal one found so far. The suggested evaluation makes use of a modified version of the sine and cosine functions, with the cosine function modelling for the process of exploring the space of possible solutions and the sine function modelling for the process of extracting the maximum value from those solutions. The following are the proposed optimization steps:

A. Initialization:

1- P-size random population (X) with a starting solution $X_k = [x_{k1}, x_{k2}, x_{k3}, \ldots, x_{kn}]$ where $k\varepsilon(1,P)$

2- Create $X\prime$, the opposite population using the (9)

$$x\prime_{ki} = u_k + v_k - x_{ki} \tag{9}$$

where i=1,2,3…,n

where (u_k, v_k) represent the solution's upper and lower bounds, respectively, i.e., $x\ \varepsilon[u,v]$, and x_{ki} represent the kth point of the ith solution.

3- To create a new population, choose the best P solutions arising from the combination of two pre-existing populations, i.e., $X \bigcup X\prime$.

B. Updated Stage:

1- The best Y solution is found from the best P solutions generated in the initial stage.

2- The SCA [24] is used to update the solutions in population, X, and their fitness functions are calculated. Using the OBL [30], the opposite population, $X\prime$, is also calculated, along with the fitness function for each $x\prime$.

3- Repeat the preceding stages until an acceptable solution is obtained.

4- Return the optimal solution found.

Fig. 7 shows the methodology for the OB-SCA algorithm, which is the proposed optimization method.

6. Results and discussion

Matlab/Simulink is used to run simulations of the WEGS model in order to provide evidence of the effectiveness of the suggested topology. Fig. 8 shows how a reference wave pattern is generated in SV-PWM technique. In Table 2,

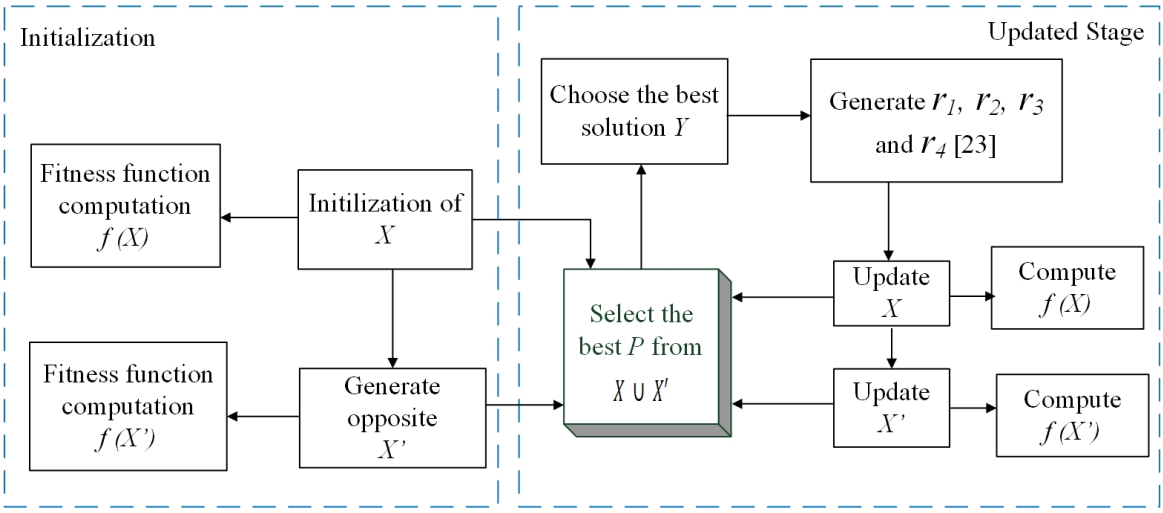

Figure 7. Two-stage OB-SCA optimization technique.

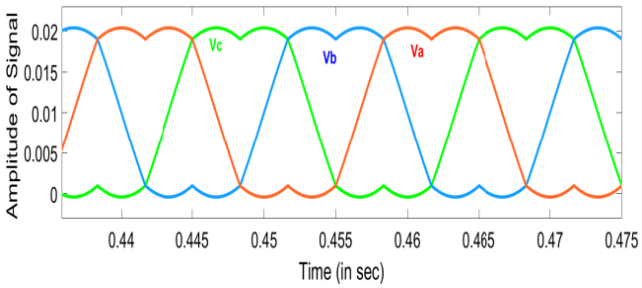

Figure 8. SV-PWM switching pattern.

Table 2. Wind turbine, PMSG, and rectifier simulation parameters.

Parameters	Value
Wind Turbine	
Power	8.5 kW
Base wind speed	12 m/s
Diameter	2.6 m
PMSG	
Rotor Speed	2032 rpm
Electrical power extracted by PMSG	4. 3 kW
Rectifier	
Rectifier Output Voltage, V_S	120 V
Rectifier Filter Inductor, L_R	23 mH
Rectifier Filter Capacitor, C_R	180 μF

Table 3. The ZSI parameters [31]

Parameters	Value
Input DC voltage, V_S	120 V
Impedance network Capacitor, C_Z	470 μF
Impedance network Inductor, L_Z	1 mH
ZSI filter capacitor	800 μF
ZSI filter inductor	900 μH
Load resistance	10 Ω
Load inductance	0.1 mH

the parameters for wind turbines, PMSG, and rectifiers are shown. The associated graph for Table 2 parameters is depicted in Fig. 9.

Table 3 shows the ZSI parameter for the proposed topology implementation.

Voltage and current waveforms at the open-loop ZSI's output without a PI controller are shown in Fig. 10, and the same graph for a closed-loop ZSI with an OB-SCA-based PI controller is shown in Fig. 11. After 1 second of simulation time, the RL load's resistance and inductance are changed from 10 ohms and 0.1 mH, respectively, to 20 ohms and 0.2 mH, and the resulting voltage and current are provided. After 1 second of simulation (when the load changes), the ZSI's output voltage rises and the current falls as the load increases (as shown in Fig. 10). In contrast, as shown in Fig. 11, the ZSI's output voltage almost remains constant as the load causes the device's output current to fall as the RL load value is increased. The output waveforms illustrate that the planned controller produces the required 210 V AC voltage constantly for the varying AC loads.

The Fast Fourier Transform (FFT) of the output voltage waveform in Fig. 12 demonstrates that the WEGS system's output waveform has a very low (0.72%) harmonic content due to the use of the SV-PWM modulation approach. The FFT analysis of output current is also shown in Fig. 13.

The objective function of the problem that is optimized is an integral square error of the difference between the impedance network capacitor voltage (V_{CZ}) and the peak of the three-phase output voltage of the inverter. ISE = $\int u^2$

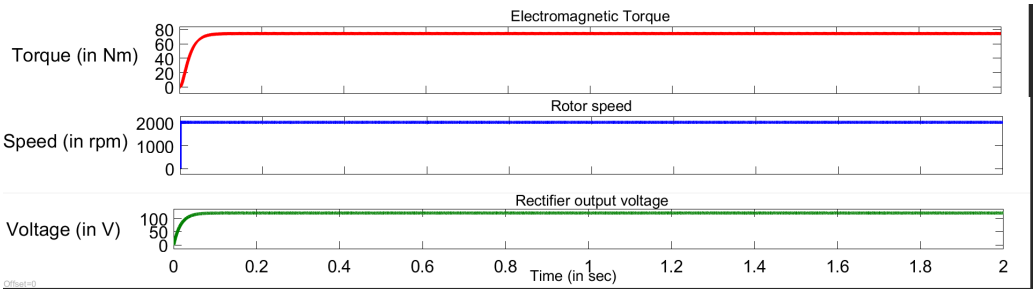

Figure 9. Waveform of electromagnetic torque of PMSG, PMSG rotor speed and rectifier output voltage after filter.

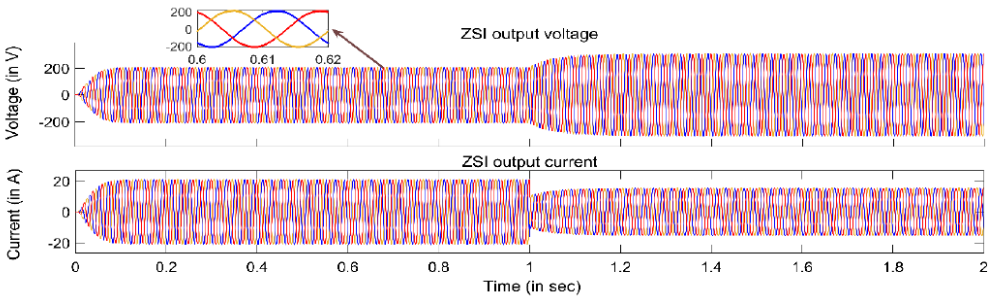

Figure 10. Uncontrolled (open-loop) ZSI output voltage and current waveform with variable RL-load.

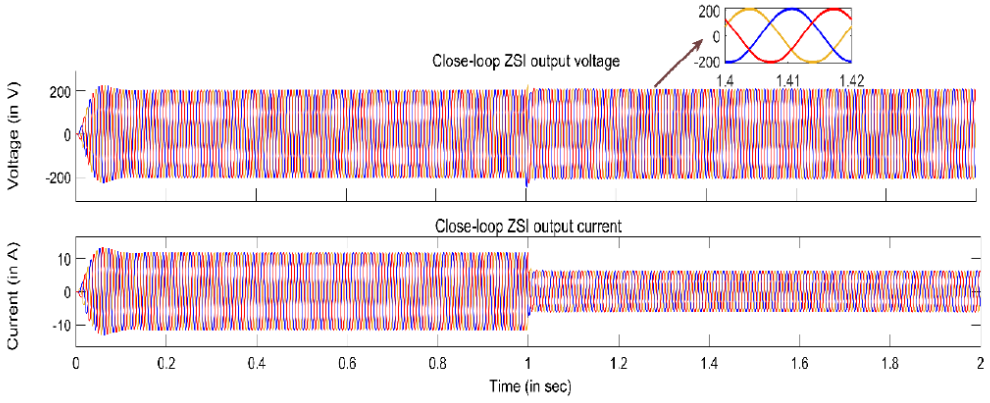

Figure 11. Controlled (close-loop) ZSI output voltage and current waveform with variable RL-load.

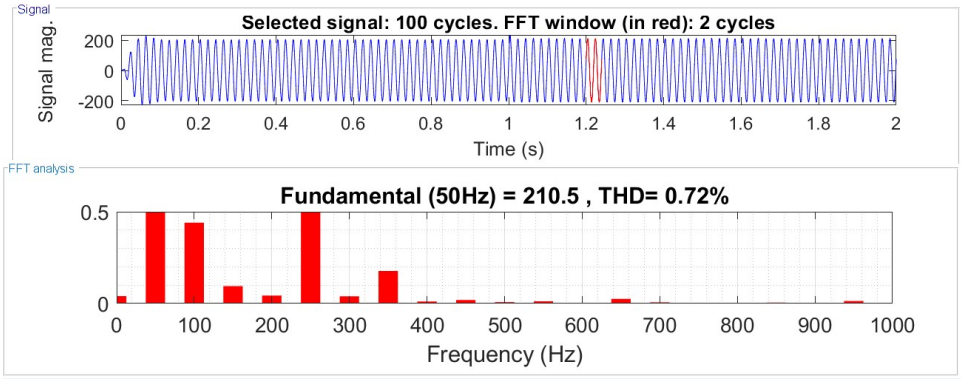

Figure 12. FFT (%THD) analysis of output voltage waveform of close-loop ZSI.

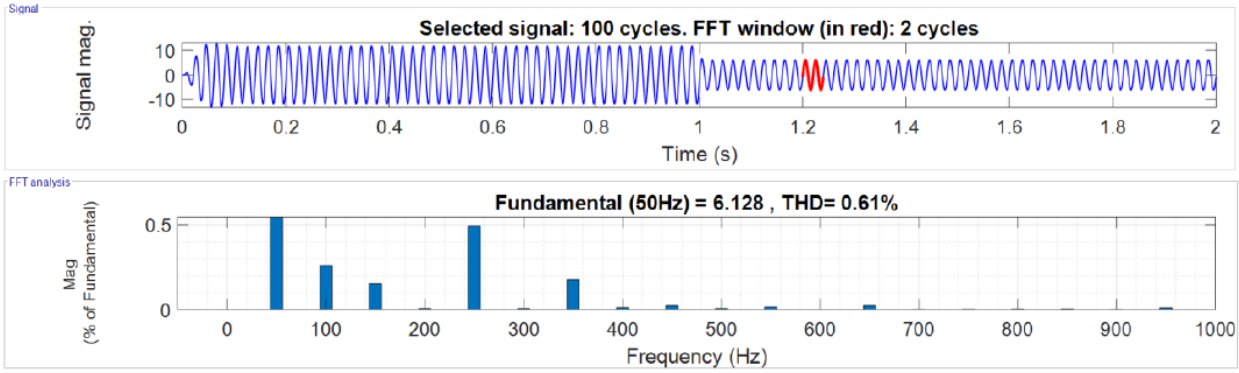

Figure 13. FFT (%THD) analysis of output current waveform of close-loop ZSI.

where u is the objective function of the problem.

Fig. 14 shows how the integral square error (ISE) of the system objective function changes as the number of iterations goes up. With better convergence at each iteration, the OB-SCA proves to be the best choice among PSO, SCA, and the OB-SCA for the suggested model. The SCA method requires three iterations to reach convergence, but the OB-SCA approach requires about five iterations. Though SCA appears to converge quickly on the convergence curve, it becomes trapped in local minima, whereas OB-SCA does not. The maximum number of iterations is chosen randomly to determine the convergence of the graph. If it does not converge after that many iterations, the number of iterations may be increased to gain better conservation observation. For the PSO method, the number of iterations required to reach convergence is 36. The linearization of the ZSI system with the controller is done, and the bode diagrams are utilised to confirm the superiority of OB-SCA further. Fig. 15 compares the bode plots of the open-loop ZSI; PSO, SCA, and OB-SCA-based closed-loop ZSI, and the relative gain margin (GM) and phase margin (PM) are compared in Table 4. By comparing the Bode diagrams of the three algorithms, the superiority of the suggested method is further confirmed. For the OB-SCA optimization technique,

Table 4. The margin of stability for the closed-loop ZSI system using various techniques.

Algorithm/ System	GM	PM
Open-loop ZSI	-23.9	-67.3
PSO	2.09	86.5
SCA	20.1	90.8
OB-SCA	35.6	90.1

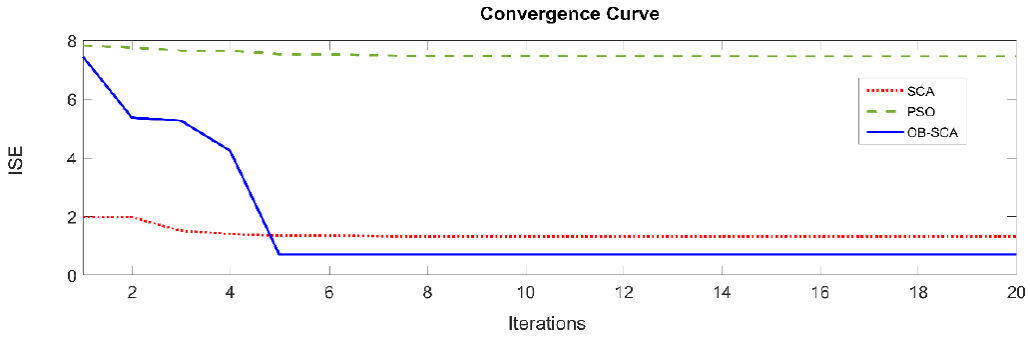

Figure 14. Graph of convergence curves for different algorithms investigated for the proposed system.

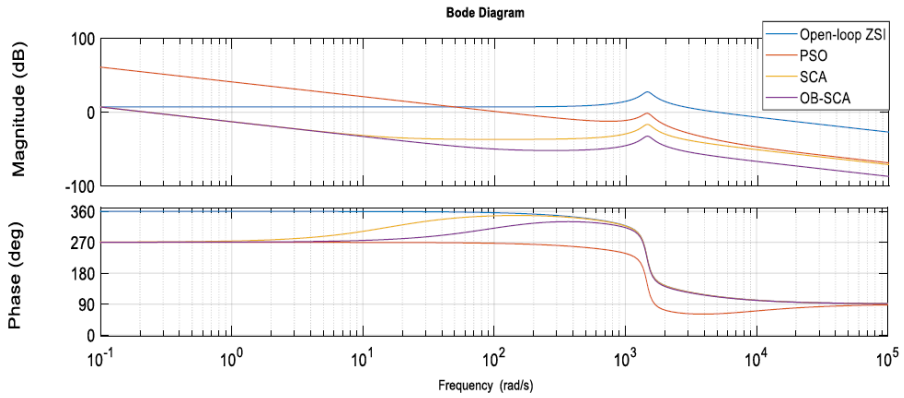

Figure 15. Bode plots of the uncontrolled ZSI and the various algorithms for the system that is proposed under test.

the control parameter values are Kp = 0.1231, and Ki = 74.4717.

7. Conclusion

In this study, a grid-connected WEGS model is constructed, which provides regulated voltage output at the load center. When compared to techniques reported in previous studies, the suggested optimal closed-loop control strategy for the ZSI is more effective in boosting the economical operation of WEGS. The voltage level between the PMSG and the load is adjusted by employing a ZSI. A MATLAB/Simulink model is utilized to assess the proposed concept. This work focused on closed-loop ZSI control via capacitor voltage control. The ZSI system's non-linearity makes PI controller parameter design difficult. Thus, this paper proposes the OB-SCA optimization method. We can conclude from theoretical and simulational analysis that the use of a PI controller makes it possible to simulate closed-loop control of a ZSI with varying three-phase RL loads. It has been observed that the OB-SCA-designed PI controller for ZSI produces more satisfying outcomes than PSO and SCA-based PI controllers. As a result, in terms of stability, the OB-SCA optimization method will be extensively used in WEGS and other emerging energy applications. The key achievements of the study are:

• The Z-source inverter's closed-loop control allows for real-time feedback and change. The system can adjust to changing operational conditions when coupled with an optimization technique, guaranteeing stability and best performance in dynamic scenarios like fluctuating loads.

• All potential solutions from the population are compared to the best solution discovered thus far using OB-SCA as an optimization technique for the closed-loop operation of ZSI. It has been noted that, compared to PSO and SCA-based PI controllers, the OB-SCA-designed PI controller for ZSI yields more satisfactory results.

An approach with high computing needs might not be appropriate in applications where real-time processing is essential.

This is the limitation of this study.
This article's long-term goal is to create a WEGS model that runs on a three-phase grid while keeping complexity and cost to a minimum.

Acknowledgement

This project would not have been feasible without the assistance of my supervisor, Dr. Rajib Kumar Mandal, who guided me through each step. I'd also like to thank a faculty member from the NIT Patna's electrical engineering department, whose great expertise and skill helped me deal with a difficult subject like "model non-linearity". I also want to thank my colleagues for sharing their knowledge and assisting me in developing my study themes.

Authors Contributions
All the authors have participated sufficiently in the intellectual content, conception and design of this work or the analysis and interpretation of the data (when applicable), as well as the writing of the manuscript.

Availability of data and materials
Data presented in the manuscript are available via request.

Conflict of Interests
The authors declare that they have no known competing financial interests or personal relationships that could have appeared to influence the work reported in this paper.

References

[1] R. Sen Subhodeep Paul, Tathagata. Dey, Pallav. Saha, and Snehasish Dey. "**Review on the development scenario of renewable energy in different country**.". *Energy Management and Renewable Resources (IEMRE)*, :pp. 44–45, 2021. DOI: https://doi.org/10.1109/IEMRE52042.2021.9386748.

[2] N. Anthony Richard and P. Navghare Seema. "**An Insight to distributed generation of electrical energy from various renewable sources**.". *International Conference on Energy Efficient Technologies for Sustainability (ICEETS)*, :pp. 341–344, 2016. DOI: https://doi.org/10.1109/ICEETS.2016.7583777.

[3] H. I. Faten Ayadi, Colak. Ilhami, and IIhan. Garip. "**Targets of countries in renewable energy**.". *International Conference on Renewable Energy Research and Applications (ICRERA)*, :pp. 394–398, 2020. DOI: https://doi.org/10.1109/ICRERA49962.2020.9242765.

[4] M. M. Bajestan, H. Madadi, , and M. A. Shamsinejad. "**Control of a new stand-alone wind turbine-based variable speed permanent magnet synchronous generator using quasi-Z-source inverter**.". *Electr. Power Syst. Res.*, 177:pp. 106010, 2019. DOI: https://doi.org/10.1016/j.epsr.2019.106010.

[5] O. Ellabban and H. Abu-Rub. "**Z-source Inverter: topology improvements review**.". *IEEE Ind. Electron. Mag.*, 10:pp. 6–24, 2016. DOI: https://doi.org/10.1109/MIE.2015.2475475.

[6] A. S. Siddhartha, G. Carl, others, and A. Azeez Najath. "**Modeling, design, control, and implementation of a modified Z-source integrated PV/Grid/EV DC charger/inverter**.". *IEEE Trans. Ind. Electron.*, 65:pp. 5213–5220, 2018. DOI: https://doi.org/10.1109/TIE.2017.2784396.

[7] Y. P. Siwakoti, F. Z. Peng, F. Blaabjerg, P. C. Loh, G. E. Town, and S. Yang. "**Impedance-source networks for electric power conversion part ii: review of control and modulation techniques**.". *IEEE Trans. Power Electron.*, 30:pp. 1887–1906, 2015. DOI: https://doi.org/10.1109/TPEL.2014.2329859.

[8] R. M. Malathi R. "**Comparison of PV based embedded Z-source inverter fed three phase induction motor with PI controller and PID controller based closed loop systems**.". , 2017. DOI: https://doi.org/10.1109/AEEICB.2017.7972400.

[9] G. Shiva, K. Hrishikes, and R. I. Raj. "**Closed loop voltage mode control of impedance source inverter (ZSI)**.". *Int. Conf. Emerg. Trends VLSI, Embed. Syst. Nano Electron. Telecommun. Syst. ICEVENT*, , 2013. DOI: https://doi.org/10.1109/ICEVENT.2013.6496528.

[10] S. Kumaravel, V. Thomas, S. K. Tripathy, and S. Ashok. "**Performance analysis of a Z-Source inverter with controller for autonomous system application**.". *IEEE 7th Int. Conf. Power Energy, PECon*, :pp. 355–359, 2018. DOI: https://doi.org/10.1109/PECON.2018.8684183.

[11] A. R. Yılmaz, B. Erol, A. Delibaşı, and B. Erkmen. "**Design of gain-scheduling PID controllers for Z-source inverter using iterative reduction-based heuristic algorithms**.". *Simul. Model. Pract. Theory.*, 94:pp. 162–176, 2019. DOI: https://doi.org/10.1016/j.simpat.2019.02.005.

[12] Ö. Özkara and A. Karaarsalan. "**Continuous time least square PI control method for quasi-Z source inverter**.". *Teh. Vjesn.*, 30:pp. 1088–1095, 2023. DOI: https://doi.org/10.17559/TV-20221104195058.

[13] R. A. Krohling and J. P. Rey. "**Design of optimal disturbance rejection PID controllers using genetic algorithms**.". *IEEE Trans. Evol. Comput.*, 5:pp. 78–82, 2001. DOI: https://doi.org/10.1109/4235.910467.

[14] J. S. Chiou, S. H. Tsaia, and M. T. Liu. "**A PSO-based adaptive fuzzy PID-controllers**.". *Simul. Model. Pract. Theory.*, 26:pp. 49–59, 2012. DOI: https://doi.org/10.1016/j.simpat.2012.04.001.

[15] P. B. De Moura Oliveira. "**Modern heuristics review for PID control systems optimization: A teaching experiment**.". *Proc. 5th Int. Conf. Control Autom. ICCA'05*, :pp. 828–833, 2005. DOI: https://doi.org/10.1109/icca.2005.1528237.

[16] M. N. Ab Wahab, S. Nefti-Meziani, and A. Atyabi. "**A comprehensive review of swarm optimization algorithms**.". *PLoS One*, 10, 2015. DOI: https://doi.org/10.1371/journal.pone.0122827.

[17] Y. F. Zou, J. Zhao, and Z. M. Gao. "**Guaranteed convergence sine cosine algorithm**.". *ACM Int. Conf. Proceeding Ser.*, :pp. 986–990, 2021. DOI: https://doi.org/10.1145/3501409.3501586.

[18] W. Long, T. Wu, X. Liang, and S. Xu. "**Solving high-dimensional global optimization problems using an improved sine cosine algorithm**.". *Expert Syst. Appl.*, 123:pp. 108–126, 2019. DOI: https://doi.org/10.1016/j.eswa.2018.11.032.

[19] S. Gupta and K. Deep. "**Improved sine cosine algorithm with crossover scheme for global optimization**.". *Knowledge-Based Syst.*, 165:pp. 374–406, 2019. DOI: https://doi.org/10.1016/j.knosys.2018.12.008.

[20] Y. P. Siwakoti, F. Z. Peng, F. Blaabjerg, P. C. Loh, , and G. E. Town. "**Impedance-source networks for electric power conversion part i: A topological review**.". *IEEE Trans. Power Electron.*, 30:pp. 699–716, 2015. DOI: https://doi.org/10.1109/TPEL.2014.2313746.

[21] S. Kumari and R. K. Mandal. "**Effectivness of space vector PWM in three-phase inverter**.". *Int. Conf. Emerg. Front. Electr. Electron. Technol. ICEFEET.*, :pp. 2–6, 2020. DOI: https://doi.org/10.1109/ICEFEET49149.2020.9187000.

[22] M. T. Islam and S. I. Ayon. "**Performance analysis of three-phase inverter for minimizing total harmonic distortion using space vector pulse width modulation technique**.". *ICCIT* 2020 – 23*rd Int. Conf. Comput. Inf. Technol. Proc.*, :pp. 14–17, 2020. DOI: https://doi.org/10.1109/ICCIT51783.2020.9392687.

[23] S. K. Baksi and R. K. Behera. "**Reduced CMV SVPWM scheme for three-level Z-source NPC inverter for PV grid integration**.". *Int. Conf. Power Electron. Energy.*, :pp. 1–6, 2023. DOI: https://doi.org/10.1109/ICPEE54198.2023.10060515.

[24] S. Mirjalili. "**SCA: a sine cosine algorithm for solving optimization problems**.". *Knowledge-Based Syst.*, 96:pp. 120–133, 2016. DOI: https://doi.org/10.1016/j.knosys.2015.12.022.

[25] M. Wang and G. Lu. "**A modified sine cosine algorithm for solving optimization problems**.". *IEEE Access*, 9:pp. 27434–27450, 2021. DOI: https://doi.org/10.1109/ACCESS.2021.3058128.

[26] P. C. Chiu, A. Selamat, O. Krejcar, and K. K. Kuok. "**Hybrid sine cosine and fitness dependent optimizer for global optimization**.". *IEEE Access*, 9:pp. 128601–128622, 2021. DOI: https://doi.org/10.1109/ACCESS.2021.3111033.

[27] S. Oshnoei, A. Oshnoei, A. Mosallanejad, , and F. Haghjoo. "**Novel load frequency control scheme for an interconnected two-area power system including wind turbine generation and redox flow battery**.". *Int. J. Electr. Power Energy Syst.*, 130:pp. 107033, 2021. DOI: https://doi.org/10.1016/j.ijepes.2021.107033.

[28] S. Padmanaban and others. "**A novel modified sine-cosine optimized MPPT algorithm for grid integrated PV system under real operating conditions**.". *IEEE Access*, 7:pp. 10467–10477, 2019. DOI: https://doi.org/10.1109/ACCESS.2018.2890533.

[29] M. Abd Elaziz, D. Oliva, and S. Xiong. "**An improved opposition-based sine cosine algorithm for global optimization**.". *Expert Syst. Appl.*, 90:pp. 484–500, 2017. DOI: https://doi.org/10.1016/j.eswa.2017.07.043.

[30] E. Cuevas, D. Oliva, D. Zaldivar, and G. Pajares. "**Opposition-based electromagnetism-like for global optimization**.". *Int. J. Innov. Comput. Inf. Control.*, 8:pp. 8181–8198, 2012. DOI: https://doi.org/10.48550/arXiv.1405.5172.

[31] A. Taheri, J. A. Bolaghi, and M. H. Babaei. "**LC-Z-source inverter design and control**.". *Chinese J. Electron.*, 29, 2020. DOI: https://doi.org/10.1049/cje.2020.03.014.